Multiwavelets on the interval and divergence-free wavelets

J. Lakey[a] and M.C. Pereyra[b]

[a] Department of Mathematical Sciences,
New Mexico State University
Las Cruces, NM 88003-8001 USA

[b]Department of Mathematics and Statistics
University of New Mexico
Albuquerque, NM 87131-1141 USA

ABSTRACT

This manuscript gives a construction of divergence-free multiwavelets which combines the Hardin-Marasovich (HM) construction with a recipe of Strela for increasing or decreasing regularity of biorthogonal wavelets. Strela's process preserves symmetry of the HM wavelets. This enables the divergence-free wavelets to be suitably adapted to the analysis of divergence-free vector fields whose boundary traces are tangent vectors.

Keywords: multiwavelets, divergence-free, Navier-Stokes

1. INTRODUCTION

When modelling physical phenomena using elementary "building block" functions, it is reasonable to require that the building blocks live in the same space as the phenomena they are being used to model. Wavelets and variations thereof have been used for turbulence modelling and solving Navier-Stokes equations which govern the velocity of an incompressible fluid.[1] The wavelets should be divergence-free to reflect incompressibility of the fluid and such wavelets have been utilized in work of Federbush[2] and of Urban[3] among others. Orthogonal, divergence-free wavelets were invented by Battle and Federbush.[4] The Battle-Federbush wavelets were used by Federbush/Cannone to build solutions of Navier-Stokes in three space dimensions, provided the initial data lies in an amenable function space. One key aspect of this work involved expressing the Leray projection in terms of the wavelets. Those wavelets have exponential decay but not compact support. In fact, it is impossible for orthogonal, divergence-free wavelets to have compact support as Lemarié showed[5].[6] Fortunately, Lemarié[7] found a way to build biorthogonal wavelets with compact support such that the reconstructing wavelet family is divergence-free. Modifications and extensions of this approach have been carried out by Urban,[3] where such wavelets have also been used to solve Navier-Stokes equations, including finding solutions on bounded domains. In fact, our future plan is to use the wavelets developed herein to solve initial-boundary value problems for Navier-Stokes for corresponding function spaces on bounded domains. In this case compact support of the wavelets will be crucial. The fact that the wavelets must then be biorthogonal may pose nontrivial issues because the Galerkin projection onto the divergence-free component will not exactly correspond to the Leray projection. These issues, however, will be addressed in later work.

The main goal of the present work is to develop a family of divergence-free wavelets, more specifically, multiwavelets, possessing what we regard to be the best possible tradeoffs between localization, smoothness, and so forth when it comes to numerical implementation and modelling of fluids. The main properties that are desired of wavelets are short support, vanishing moments, and smoothness. The competition between these properties is well-documented. The DGHM multiwavelets[8] are in some sense optimal as regards these properties, at least in circumstances where Lipschitz continuity is adequate. Furthermore, the DGHM wavelets are symmetrical, and so provide a simple way of getting at boundary behavior compared to standard wavelets. The divergence-free wavelets here are built by adapting Lemarié's notion of MRA's related by differentiation to the setting of a class of DGHM-type biorthogonal multiwavelets whose properties were investigated by Hardin and Marasovich.[9] The key tool is a

Email for JL: jlakey@nmsu.edu; Email for MCP: crisp@math.unm.edu;
Both authors were supported by a Sandia Labs SURP grant

result in Strela's thesis.[10] We then use tensor products to factor in the divergence-free property. This means that certain combinations of the wavelets are smoothed in specific coordinates. Tensor products are a good way of building vanishing moments into multidimensional wavelets. The tradeoff is the issue of dimensionality. The divergence-free vector field basis that we construct in two dimensions has twelve wavelet mothers. In three dimensions there would be 112. In other words, we must implement the cascade algorithm a large number of times to compute the divergence-free projection defined by the wavelets. While this sounds bad, in terms of modelling it really is not. As one can see in Figure 6, the various mother wavelet vector fields have outstanding characteristics regarding tradeoff between *spatial localization* and *spatial orientation*. Consequently we are optimistic that these wavelet fields will provide a significant processing gain relative to other techniques as regards tracking of vortices and their interactions.

2. HARDIN-MARASOVICH WAVELETS

2.1. Dual families and coefficients

In the work of Geronimo Hardin and Massopust, and later of Hardin and Marasovich,[9] scaling vectors were constructed based on fractal interpolation techniques. Biorthogonal multiresolution analyses could then be constructed essentially by using a biorthogonal Gram-Schmidt process. We will use the *HM multiwavelets* to build biorthogonal divergence-free wavelets. More information about the construction of the wavelets and how it can be generalized, as well as the smoothing and roughening process that gives rise to the divergence-free wavelets, can be found in [11]. Here we will summarize the construction.

We will use the notation $\frac{1}{2}\Phi(\frac{x}{2}) = \sum C_k \Phi(x-k)$ and $\frac{1}{2}\Psi(\frac{x}{2}) = \sum D_k \Phi(x-k)$ to denote the fundamental scaling and wavelet equations. The *scaling vector* is $\Phi(x) = [\phi_1(x), \phi_2(x)]^T$ and the wavelet vector is $\Psi(x) = [\psi_1(x), \psi_2(x)]^T$. The coefficients C_k and D_k are two-by-two matrices. When one imposes among the HM family the constraint that the scaling functions and wavelets should be symmetric, as we do here, the coefficients for the HM scaling and wavelet filters will depend on a parameter s. Furthermore, the parameter $\tilde{s}$ that is used to denote the biorthogonal MRA will be related to the parameter s for the original MRA by

$$\tilde{s} = \frac{1+2s}{5s-2}.$$

Continuity and approximation properties of the scaling/wavelet vectors depend on the values of s. The scaling filter, or transfer function, is a matrix with polynomial entries $H_s(z) = \sum C_k(s) z^k$ where the C_k are the two-by-two scaling matrices with entries depending on the parameter s. The corresponding high pass or wavelet filter has the form $F_s(z) = \sum D_k(s) z^k$. Everything is set up so that the filters for the scaling and wavelet functions in the multiresolution analysis biorthogonal to that generated by $H_s(z)$ have the form $H_{\tilde{s}}(z)$ and $F_{\tilde{s}}(z)$ respectively. Because we want to build differentiation into this scale of biorthogonal multiresolution analyses, we shall choose our filter coefficients with a normalization slightly different from that given in [9]. The coefficients are listed in Table 2.1.

Table 2.1: HM scaling and wavelet coefficients

j	scaling coefficient $C_j(s)$	wavelet coefficient $D_j(s)$
-2	$\frac{1}{24}\begin{bmatrix} 0 & -(1+2s)\sqrt{2} \\ 0 & 0 \end{bmatrix}$	$\frac{1}{24}\begin{bmatrix} 0 & -(1+2s)\sqrt{2} \\ 0 & -(2+4s) \end{bmatrix}$
-1	$\frac{1}{24}\begin{bmatrix} -2+8s & (5-2s)\sqrt{2} \\ 0 & 0 \end{bmatrix}$	$\frac{1}{24}\begin{bmatrix} -2+8s & (5-2s)\sqrt{2} \\ \sqrt{2}(-2+8s) & 10-4s \end{bmatrix}$
0	$\frac{1}{24}\begin{bmatrix} 12 & (5-2s)\sqrt{2} \\ 0 & 8+4s \end{bmatrix}$	$\frac{1}{24}\begin{bmatrix} -12 & (5-2s)\sqrt{2} \\ 0 & 4s-10 \end{bmatrix}$
1	$\frac{1}{24}\begin{bmatrix} -2+8s & -(1+2s)\sqrt{2} \\ 8\sqrt{2}(1-s) & 8+4s \end{bmatrix}$	$\frac{1}{24}\begin{bmatrix} -2+8s & -(1+2s)\sqrt{2} \\ \sqrt{2}(2-8s) & 2+4s \end{bmatrix}$

In Figures 1–3 we plot the HM scaling functions and wavelets (shifted by two units) for a few values of the parameter s. Notice that they are piecewise linear when $s = 0$. In general, those functions are Lipschitz continuous of order α if $|s| < 2^{-\alpha}$, but can be discontinuous for $|s| \geq 1$. They become piecewise smooth as $s \to 2/5^-$ but their

duals, while still having compact support, become distributions of increasingly higher order. The orthogonal cases correspond to $s = 1$ and $s = -1/5$: the DGHM case. The functions are not continuous when $s = 1$ though they are piecewise linear in that case. In what follows we shall always assume that $|s| \leq 1/2$ and we will usually take $s = 0$.

2.2. Filters and Biorthogonality

With the coefficients in Table 2.1, the biorthogonal scaling and wavelet filters then have the respective forms:

$$\begin{aligned} H_s(z) &= \frac{1}{24z^2}\begin{bmatrix} 12z^2 + (8s-2)(z+z^3) & \sqrt{2}[(5-2s)(z+z^2) - (1+2s)(1+z^3)] \\ 8\sqrt{2}(1-s)z^3 & (8+4s)(z^2+z^3) \end{bmatrix} \\ H_{\tilde{s}}^*(z) &= \frac{z^2}{24(5s-2)}\begin{bmatrix} \frac{6}{z}\left(s+2+\frac{10}{z}s-\frac{4}{z}+\frac{1}{z^2}s+\frac{2}{z^2}\right) & \frac{24}{z^3}\sqrt{2}(s-1) \\ 3\sqrt{2}\left(\frac{10}{z}s-\frac{4}{z}-\frac{3}{z^2}s-3s\right)\left(1+\frac{1}{z}\right) & \frac{12}{z^2}(4s-1)\left(1+\frac{1}{z}\right) \end{bmatrix} \end{aligned}$$

$$\begin{aligned} F(z) &= \frac{1}{24z^2}\begin{bmatrix} (8s-2)(z+z^3) - 12z^2 & \sqrt{2}[(5-2s)(z+z^2) - (1+2s)(1+z^3)] \\ \sqrt{2}(8s-2)(z-z^3) & (4s-10)(z^2-z) + (2+4s)(z^3-1) \end{bmatrix} \\ F_{\tilde{s}}^*(z) &= \frac{z^2}{24(5s-2)}\begin{bmatrix} (6s+12)\left(\frac{1}{z}+\frac{1}{z^3}\right) + (24-60s)\frac{1}{z^2} & \sqrt{2}(s+2)\left(\frac{6}{z}-\frac{6}{z^3}\right) \\ \left(\frac{3}{z}+\frac{3}{z^2}\right)(7s-4)\sqrt{2} - 9s(1+\frac{1}{z^3})\sqrt{2} & 18s(\frac{1}{z^3}-1) + (42s-24)\left(\frac{1}{z}-\frac{1}{z^2}\right) \end{bmatrix}. \end{aligned}$$

Here, $L^*(z) = L^T(1/z)$. It is well-known that the condition that the scaling functions and wavelets give rise to biorthogonl MRA's can be encoded completely in terms of the filters (see Strela[10]). These conditions are summarized in Table 2.2. They are best checked with the aid of a symbolic computational tool such as Maple.

Table 2.2: Conditions of Biorthogonality
$H_s(z)H_{\tilde{s}}^*(z) + H_s(z)H_{\tilde{s}}^*(-z) = I$
$F_s(z)F_{\tilde{s}}^*(z) + F_s(z)F_{\tilde{s}}^*(-z) = I$
$H_s(z)F_{\tilde{s}}^*(z) + H_s(z)F_{\tilde{s}}^*(-z) = 0$
$F_s(z)H_{\tilde{s}}^*(z) + F_s(z)H_{\tilde{s}}^*(-z) = I$

3. SMOOTHING AND ROUGHENING

3.1. Two-scale transform

Lemarié[7] showed that given a pair of biorthogonal scalar MRAs – that is, ones generated by a single scaling function as opposed to multiple ones – with sufficient regularity, one could build from these another pair such that the derivatives of the new wavelets are essentially the original wavelets. In his thesis, Strela found a technique that amounts to the multiwavelet version of Lemarié's technique. In the scalar case the trick is to add a zero to the dual low pass filter at $z = -1$. This is equivalent to multiplying the dual low pass filter by $\frac{1+z}{2}$. In the multiwavelet setup the low-pass filter is vector-valued and the analogous procedure amounts to adding an eigenvalue zero to the low pass filter at $z = -1$ in an appropriate manner. As is typical of multiwavelets, there is some flexibility in carrying out this extension of Lemarié's method. The method is encoded in Strela's *two-scale transform*. It amounts to finding a suitable *transition matrix* M and then forming the new low pass filter $H_+(z) = \frac{1}{2}M^*(z^2)\tilde{H}(z)M^{*-1}(z)$. Thereby, M accomplishes a transition between a pair of two-scale MRAs. In the scalar MRA case, the role of M^* is played by $1 - z$; the property desired of M^* is that it has a simple eigenvalue zero at $z = 1$ whose eigenvector is shared with the unit eigenvalue of $\tilde{H}(1)$. Existence of the latter is guaranteed by the scaling property of $\tilde{H}$. Further issues in the design of M include preservation of symmetries and compact support. These issues are discussed in Strela's thesis[10] and some recent work of the authors[11]; for example, the fact that the smoothing and roughening operators in Table 3.1 are related by taking adjoints depends on symmetry. Those considerations led to the particular choice of M that we use below. Actually, our particular normalization of the HM wavelets allows us to use a single matrix

Table 3.1: Smoothened and roughened MRAs		
smoothened scaling	$H_+(z) = \frac{1}{2}M^*(z^2)\tilde{H}(z)M^{*-1}(z)$	$\frac{d}{dx}\Phi_+(x) = -T_{M^*}\Phi(x)$
roughened scaling	$H_-(z) = 2M^{-1}(z^2)H(z)M(z)$	$\frac{d}{dx}\Phi(x) = T_M\Phi_-(x)$
smoothened wavelet	$F_+(z) = \frac{1}{2}\tilde{F}(z)M^{*-1}(z)$	$\frac{d}{dx}\Psi_+(x) = -\Psi(x)$
roughened wavelet	$F_-(z) = 2F(z)M(z)$	$\frac{d}{dx}\Psi(x) = \Psi_-(x)$

M for any value of the HM parameter s. Table 3.1 summarizes the procedure for forming the new families of dual MRA's. It also records the relationships between the smoothed and roughened filters.

It is a simple matter to check that the conditions of biorthogonality are preserved. For example, one has

$$\begin{aligned} H_+(z)H_-^*(z) &= \left[\frac{1}{2}M^*(z^2)\tilde{H}(z)M^{*-1}(z)\right]\left[2M^{-1}(z^2)H(z)M(z)\right]^* \\ &= M^*(z^2)\tilde{H}(z)H^*(z)M^{*-1}(z^2) \end{aligned}$$

so that, $\tilde{H}(z)H^*(z) + \tilde{H}(-z)H^*(-z) = I$ implies

$$H_+(z)H_-^*(z) + H_+(-z)H_-^*(-z) = M^*(z^2)\left[\tilde{H}(z)H^*(z) + \tilde{H}(-z)H^*(-z)\right]M^{*-1}(z^2) = I$$

The other conditions are similarly verified. The operator T_{M^*} is an an operator-valued matrix whose entries are polynomials in the shift operator. Its symbol is M^*. *So at the level of wavelets this process really amounts to integrating or differentiating the wavelet components!*

3.2. Eigenvectors and the Transition matrix

The matrix $H_s(1) = \frac{1}{3}\begin{bmatrix} 1+2s & \sqrt{2}(1-s) \\ \sqrt{2}(1-s) & 2+s \end{bmatrix}$ has eigenvalues s and 1. For $\lambda = 1$ the corresponding eigenvector is $\begin{bmatrix} \alpha & \beta \end{bmatrix}^T = \alpha \begin{bmatrix} 1 & \sqrt{2} \end{bmatrix}^T$ *independent of* s. One easily checks that for the matrix $M^*(z) = \begin{bmatrix} 0 & 1-\frac{1}{z} \\ 2\sqrt{2} & -\frac{1}{z}-1 \end{bmatrix}$, $\begin{bmatrix} 1 & \sqrt{2} \end{bmatrix}^T$ generates the kernel for $M^*(1)$ so Strela's eigenvector criterion is satisfied. Up to multiplication by z^k this is the unique transition matrix that preserves symmetry and increases the support of the HM scaling vector – that is, the sum of the supports of its components – by one.

3.3. Smoothed and roughened HM filters

We emphasize here that the smoothing transition is applied to the $\tilde{s}$ filter while the roughening transition is applied to the s filter. Then the recipe for smoothing and roughening the filters yields:

$$\begin{aligned} H_{s,+}(z) &= \frac{1}{2}M^*(z^2)H_{\tilde{s}}(z)M^{*-1}(z) \\ &= \left\{\frac{1}{z}\begin{bmatrix} \frac{1}{4} & \frac{(1-s)}{4(5s-2)} \\ \frac{3}{8} & \frac{(4-s)}{8(5s-2)} \end{bmatrix} + \begin{bmatrix} \frac{1}{2} & 0 \\ 0 & \frac{1}{4} \end{bmatrix} + z\begin{bmatrix} \frac{1}{4} & \frac{(s-1)}{4(5s-2)} \\ -\frac{3}{8} & \frac{(4-s)}{8(5s-2)} \end{bmatrix}\right\} \end{aligned}$$

$$\begin{aligned} H_{s,-}(z) &= 2M^{-1}(z^2)H_s(z)M(z) \\ &= \frac{1}{12z^2}\left\{\begin{bmatrix} -\frac{1}{2}-s & \frac{1}{2}+s \\ -\frac{1}{2}-s & \frac{1}{2}+s \end{bmatrix} + z\begin{bmatrix} 3 & -4+10s \\ 3 & -4+10s \end{bmatrix} + z^2\begin{bmatrix} 7+2s & 0 \\ 0 & 7+2s \end{bmatrix}\right. \\ &\qquad \left. + z^3\begin{bmatrix} 3 & 4-10s \\ -3 & 10s-4 \end{bmatrix} + z^4\begin{bmatrix} -\frac{1}{2}-s & -\frac{1}{2}-s \\ \frac{1}{2}+s & \frac{1}{2}+s \end{bmatrix}\right\} \end{aligned}$$

3.4. Smoothed and roughened wavelets

Here we use the recipe $F_+(z) = \frac{1}{2}\tilde{F}(z)M^{*-1}(z)$ and $F(z) = \frac{1}{2}F_-(z)M^{-1}(z)$ to obtain

$$F_+(z) = \frac{1}{2}\begin{bmatrix} -\frac{1}{16}\frac{\sqrt{2}}{z}\left(z^2-1\right) & \frac{1}{16z}\left(z^2s+2z^2-10zs+4z+s+2\right)\frac{\sqrt{2}}{5s-2} \\ \frac{1}{8}\frac{z^2-2z+1}{z} & -\frac{1}{8z}\left(s+2\right)\frac{z^2-1}{5s-2} \end{bmatrix}$$

$$F_-(z) = \begin{bmatrix} \frac{1}{12}\sqrt{2}\left(z^2+2z^2s-6z+1+2s\right)\frac{z^2-1}{z^2} & \frac{\sqrt{2}}{12}\frac{(20s-8)(z+z^3)+(1+2s)(1+z^4)+(4s-34)z^2}{z^2} \\ -\frac{1}{6}\left(z-1\right)^2\frac{2z^2s+z^2+4zs-4z+2s+1}{z^2} & -\frac{1}{6}\frac{8z-20zs-8z^3+20z^3s-1-2s+z^4+2z^4s}{z^2} \end{bmatrix}$$

Figure 4 shows shifted versions of the smoothed and roughened dual scaling functions and wavelets for the special case where $s = 0$. In reality, the first components of the smoothed and roughened filters are symmetric about $x = 0$ whereas the second components are both antisymmetric about $x = 0$. It is not obvious from the filter equations that the scaling supports should all have length two: this ultimately depends on some subtle cancellation properties among the components. It is, however, easy to see that the differentiation property holds, especially that the derivatives of the $s = 0$ wavelets really are what we are calling the roughened wavelets. In Table 3.4, k is running from $k = -2$ in the top row to $k = 2$ in the bottom row.

Table 3.4: Smoothed and roughened scaling and wavelet coefficients

smooth scaling $C_k^+(s)$	smooth wavelet $D_k^+(s)$	rough scaling $C_k^-(s)$	rough wavelet $D_k^-(s)$
$\begin{bmatrix} 0 & 0 \\ 0 & 0 \end{bmatrix}$	$\begin{bmatrix} 0 & 0 \\ 0 & 0 \end{bmatrix}$	$\frac{1}{12}\begin{bmatrix} -\frac{1}{2}-s & \frac{1}{2}+s \\ -\frac{1}{2}-s & \frac{1}{2}+s \end{bmatrix}$	$\frac{1+2s}{12}\begin{bmatrix} -\sqrt{2} & \sqrt{2} \\ -2 & 2 \end{bmatrix}$
$\begin{bmatrix} \frac{1}{4} & \frac{(1-s)}{4(5s-2)} \\ \frac{3}{8} & \frac{(4-s)}{8(5s-2)} \end{bmatrix}$	$\begin{bmatrix} \frac{\sqrt{2}}{32} & \frac{\sqrt{2}}{32}\frac{2+s}{5s-2} \\ \frac{1}{16} & \frac{1}{16}\frac{s+2}{(5s-2)} \end{bmatrix}$	$\frac{1}{12}\begin{bmatrix} 3 & -4+10s \\ 3 & -4+10s \end{bmatrix}$	$\frac{1}{12}\begin{bmatrix} 6\sqrt{2} & \sqrt{2}(20s-8) \\ 12 & 40s-16 \end{bmatrix}$
$\begin{bmatrix} \frac{1}{2} & 0 \\ 0 & \frac{1}{4} \end{bmatrix}$	$\begin{bmatrix} 0 & -\frac{1}{16}\sqrt{2} \\ -\frac{1}{8} & 0 \end{bmatrix}$	$\frac{1}{12}\begin{bmatrix} 7+2s & 0 \\ 0 & 7+2s \end{bmatrix}$	$\frac{1}{12}\begin{bmatrix} 0 & \sqrt{2}(4s-34) \\ 8s-20 & 0 \end{bmatrix}$
$\begin{bmatrix} \frac{1}{4} & \frac{(s-1)}{4(5s-2)} \\ -\frac{3}{8} & \frac{(4-s)}{8(5s-2)} \end{bmatrix}$	$\begin{bmatrix} -\frac{\sqrt{2}}{32} & \frac{\sqrt{2}}{32}\frac{s+2}{5s-2} \\ \frac{1}{16} & -\frac{1}{16}\frac{s+2}{(5s-2)} \end{bmatrix}$	$\frac{1}{12}\begin{bmatrix} 3 & 4-10s \\ -3 & 10s-4 \end{bmatrix}$	$\frac{1}{12}\begin{bmatrix} -6\sqrt{2} & \sqrt{2}(20s-8) \\ 12 & 16-40s \end{bmatrix}$
$\begin{bmatrix} 0 & 0 \\ 0 & 0 \end{bmatrix}$	$\begin{bmatrix} 0 & 0 \\ 0 & 0 \end{bmatrix}$	$\frac{1}{12}\begin{bmatrix} -\frac{1}{2}-s & -\frac{1}{2}-s \\ \frac{1}{2}+s & \frac{1}{2}+s \end{bmatrix}$	$\frac{(1+2s)}{12}\begin{bmatrix} \sqrt{2} & \sqrt{2} \\ -2 & -2 \end{bmatrix}$

4. BASES FOR $H_0^1[0,1]$

4.1. Localized MRAs

By $H_0^1[0,1]$ we mean the Sobolev subspace of $L^2[0,1]$ defined by the closure of $C_0^\infty[0,1]$ with respect the norm $\|f\|_{H^1}^2 = \|f\|_{L^2}^2 + \|f'\|_{L^2}^2$. As mentioned, the HM wavelets $\Psi = \Psi_s$ are Lipschitz continuous provided $-1/2 \le s \le 0$,[11] hence those wavelets supported in $[0,1]$ belong to $H_0^1[0,1]$. But the symmetry properties of the wavelets give us extra leverage, ultimately showing that an appropriate subfamily of the HM wavelets forms an unconditional basis for $H_0^1[0,1]$. This fact persists for the smoothed wavelets as well but the details are a little different.[11] In contrast, here we will argue directly from the symmetry properties to show that one can get such a basis without requiring added smoothing. However, we do make reference to the roughened wavelets. The Lipschitz property is crucial because it guarantees that the roughened wavelets will still form a Riesz basis, so we shall assume that $s \in [-1/2, 0]$ is fixed and let $\Phi_s = [\phi_1, \phi_2]^T$ be the HM scaling vector and $\Psi_s = [\psi_1, \psi_2]^T$ the corresponding wavelet vector.

As is evident from Figures 1–3, for any value of s, ϕ_1 is supported in $[-1, 1]$ and is symmetric with respect to $x = 0$ while ϕ_2 is supported in $[0, 1]$ and is symmetric with respect to $x = 1/2$. For the wavelets, both ψ_i are supported in $[-1, 1]$, but ψ_1 is symmetric with respect to $x = 0$ while ψ_2 is antisymmetric. Since $\tilde{s} \in [-1/2, 0]$ when s is, the same can be said for the $\tilde{\Phi}_s$ and $\tilde{\Psi}_s$ components. To begin, recall that the functions $\phi_{ijk}(x) = 2^{j/2}\phi_i(2^j x - k)$ form a basis

for the multiresolution space V_j as $i = 1, 2$ and $k \in \mathbf{Z}$ while $\psi_{ijk}(x) = 2^{j/2}\psi_i(2^j x - k)$ form a basis for the *detail* space W_j as $i = 1, 2$ and $k \in \mathbf{Z}$. The multiresolution setup allows us to conclude that $L^2(\mathbf{R}) = V_{j_0} \oplus (\oplus_{j \geq j_0} W_j)$ for any integer j_0 where the direct sum is *oblique* (not necessarily orthogonal) in this case. The same holds for the dual MRA.

In contrast, we want to define a multiresolution expansion of functions restricted to $[0, 1]$. To do so, we will add some new notation:

$$\begin{cases} \varphi^{\mathrm{e}}_{jk}(x) = 2\phi_{ijk}(x)\chi_{[0,1]}(x), \ i = 1, \ k = 0, 2^j \text{ (symmetric)} \\ \varphi^{\mathrm{int}}_{ijk}(x) = \phi_{ijk}(x), i = 1, 2, \ k = 1, ..., 2^j - 1 \text{ or } i = 2, k = 0 \text{ (interior)} \end{cases}$$

and we take

$$\begin{cases} \omega^{\mathrm{e}}_{jk}(x) = 2\psi_{ijk}(x)\chi_{[0,1]}(x), \ i = 1, \ k = 0, 2^j \text{ (symmetric)} \\ \omega^{\mathrm{o}}_{jk}(x) = 2\psi_{ijk}(x)\chi_{[0,1]}(x), \ i = 2, \ k = 0, 2^j \text{ (antisymmetric)} \\ \omega^{\mathrm{int}}_{ijk}(x) = \psi_{ijk}(x), i = 1, 2, \ k = 1, ..., 2^j - 1 \text{ (interior)} \end{cases}$$

and the letters 'e' and 'o' stand for 'even' and 'odd'. In a sense there are two natural multiresolution subspaces for $[0, 1]$ at each level: the first is built from the interior and symmetric elements, the second is build from the interior and antisymmetric elements. All of these functions are normalized and truncated if need be to live inside of $[0, 1]$. We will use the abbreviated notation ω_{ijk} when it is clear to which restricted wavelets we are referring. For the multiresolution spaces, we let $\mathcal{V}_{j,\mathrm{e}}$ denote the span of the elements of V_j that are either interior to $[0, 1]$ *or* the restrictions of ones symmetric at the endpoints, suitably normalized, while $\mathcal{W}_{j,\mathrm{e}}$ denotes the corresponding wavelet subspace elements. We can define the antisymmetric spaces $\mathcal{V}_{j,\mathrm{o}}$ and $\mathcal{W}_{j,\mathrm{o}}$ as the span of the scaling and wavelet elements in V_j and W_j respectively that are either interior to $[0, 1]$ or the restrictions of ones antisymmetric at the endpoints, suitably normalized.

A remark about biorthogonality is in order. We can define the biorthogonal spaces $\tilde{\mathcal{V}}_{j,\mathrm{o}}$ and $\tilde{\mathcal{W}}_{j,\mathrm{o}}$ but the biorthogonality is really something to be checked. In other words we must check that, for example, $\mathcal{W}_{j,\mathrm{o}}$ and $\tilde{\mathcal{W}}_{j',\mathrm{o}}$ are indeed biorthogonal. Obviously there is no problem for the $\omega^{\mathrm{int}}_{ijk}(x)$ and $\tilde{\omega}^{\mathrm{int}}_{i'j'k'}(x)$ because this case goes back to the analysis on $L^2(\mathbf{R})$. The only conceivable problem is when both functions live at one endpoint, for example, $i = 2$ and $k = k' = 0$. But then if $\left\langle \psi^2_{j0}, \tilde{\psi}^2_{j'0} \right\rangle = 0$ then since both terms are antisymmetric it must be that $\left\langle \omega^{\mathrm{o}}_{j0}, \tilde{\omega}^{\mathrm{o}}_{j'0} \right\rangle = 0$. In fact, we have:

PROPOSITION 4.1. *$L^2[0, 1]$ is the oblique direct sum of the span of $\mathcal{V}_{1,o}$*

together with the $\mathcal{W}_{j,o}, j = 1, 2, ...$ In fact, one has

$$f = \sum_{\varphi^{int}_{i1k} \in \mathcal{V}_{j,o}} \left\langle f, \tilde{\varphi}^{int}_{i1k} \right\rangle \varphi^{int}_{i1k} + \sum_{j=1}^{\infty} \left[\sum_{\omega^{int}_{ijk} \in \mathcal{W}_{j,o}} \left\langle f, \tilde{\omega}^{int}_{ijk} \right\rangle \omega^{int}_{jk} + \sum_{\omega^{o}_{jk} \in \mathcal{W}_{j,o}} \left\langle f, \tilde{\omega}^{o}_{jk} \right\rangle \omega^{o}_{jk} \right] \tag{1}$$

with

$$\|f\|_2^2 \sim \sum_{\varphi^{int}_{i1k} \in \tilde{\mathcal{V}}_{j,o}} \left| \left\langle f, \tilde{\varphi}^{int}_{i1k} \right\rangle \right|^2 + \sum_{j=1}^{\infty} \left[\sum_{\omega^{int}_{ijk} \in \mathcal{W}_{j,o}} \left| \left\langle f, \tilde{\omega}^{int}_{ijk} \right\rangle \right|^2 + \sum_{\omega^{o}_{jk} \in \mathcal{W}_{j,o}} \left| \left\langle f, \tilde{\omega}^{o}_{jk} \right\rangle \right|^2 \right] \tag{2}$$

Proof. The idea is quite simple. First one can take the $L^2(\mathbf{R})$ expansion of f supported in $[0, 1]$ in terms of the oblique projections onto V_1 and the sum of the projections onto $W_j, j = 1, 2, ...$ That is, $f = P_{V_1} f + \sum_{j=1}^{\infty} P_{W_j} f$ as an element of $L^2(\mathbf{R})$. The interior terms of this expansion are identical with the interior terms of the expansion in the Proposition. The only difference lies in the terms in this expansion which overlap the boundary. For example, in principle the projection of f onto V_1 will live in $[-1/2, 3/2]$ even though f itself lives in $[0, 1]$. In contrast, $P_{\mathcal{V}_1} f = \sum_{\varphi^{\mathrm{int}}_{i1k} \in \mathcal{V}_{1,\mathrm{o}}} \left\langle f, \tilde{\varphi}^{\mathrm{int}}_{i1k} \right\rangle \varphi^{\mathrm{int}}_{i1k}$ is supported in $[0, 1]$. We just focus on behavior at the left endpoint $x = 0$ here. At each level $j \geq 1$ there are two wavelet terms in $P_{W_j} f$ which straddle the point $x = 0$, one of which is symmetric, the other is antisymmetric. Because f lives in $[0, 1]$ and because of the supports of the wavelets, these are the only W_j terms that can contribute to f outside of $[0, 1]$. Consequently, the sum of the antisymmetric wavelet terms straddling

$x = 0$ must *cancel* the sum of the V_1 and W_j symmetric terms that straddle $x = 0$ *outside* of $[0,1]$ and must *equal* the sum of the V_0 and W_j symmetric terms that straddle $x = 0$ *inside* of $[0,1]$. This verifies the expansion (1). The norm equivalence (2) follows simply from (i) the equivalence of the $L^2(\mathbf{R})$ norm of f and the sum of squares of coefficients in the usual wavelet expansion together with (ii) the fact that the energy encoded in the symmetric straddling terms equals the energy encoded in the antisymmetric straddling terms, and (iii) the biorthogonality of those terms. This proves the proposition. □

4.2. Convergence in $H_0^1[0,1]$

We could have equally well expanded f in terms of the symmetric and interior terms alone; however to describe $H_0^1[0,1]$ it is necessary to expand in terms of wavelets that vanish at the endpoints, which indeed happens when one uses the antisymmetric restrictions. Nevertheless, the symmetric restrictions will also play a role in boundary value problems.

COROLLARY 4.2. *The expansion (1) persists for $H_0^1[0,1]$ for which one has the norm equivalence*

$$\|f\|_{H^1}^2 \sim \sum_{\varphi_{i1k}^{int} \in \mathcal{V}_{1,o}} \left|\langle f, \tilde{\varphi}_{i1k}^{int} \rangle\right|^2 + \sum_{j=1}^{\infty} (1 + 2^{2j}) \sum_{\omega_{ijk} \in \mathcal{W}_{j,o}} \left|\langle f, \tilde{\omega}_{jk}^{i} \rangle\right|^2$$

Proof. The expansion persists because we are using the antisymmetric terms which all vanish at the endpoints. What is crucial here is that we can also differentiate the expansion to get:

$$\frac{df}{dx} = 2 \sum_{\varphi_{i1k}^{\text{int}} \in \mathcal{V}_{1,\text{o}}} \langle f, \tilde{\varphi}_{i1k}^{\text{int}} \rangle \frac{d}{dx} \varphi_{i1k}^{\text{int}} + \sum_{j=1}^{\infty} 2^j \sum_{\omega_{ijk} \in \mathcal{W}_{j,\text{o}}} \langle f, \tilde{\omega}_{ijk} \rangle \, \omega_{ijk,-}$$

where $\omega_{ijk,-}$ denotes the normalized restriction to $[0,1]$ of the corresponding ψ_{ijk-}. Now one just uses the fact that the $\frac{d}{dx}\varphi_{i1k}^{\text{int}}$ and ω_{ijk-} also form a Riesz basis for their span – which follows from the biorthgonality property of the smoothened and roughened wavelets – to verify that

$$\|f'\|_2^2 \sim \sum_{\varphi_{i1k}^{\text{int}} \in \mathcal{V}_{1,\text{o}}} \left|2 \langle f, \tilde{\varphi}_{i1k}^{\text{int}} \rangle\right|^2 + \sum_{j=1}^{\infty} 2^{2j} \sum_{\omega_{jk}^{i} \in \mathcal{W}_{j,\text{o}}} \left|\langle f, \tilde{\omega}_{jk}^{i} \rangle\right|^2 .$$

This verifies the corollary. □

Using similar arguments one can show that the assymetrical parts of the smoothened wavelets also give a norm equivalence for $H_0^1[0,1]$. This becomes useful when constructing divergence-free wavelets, so we record the result here. First we note that we can define the spaces $\mathcal{V}_{j,\text{o}}^+$ and $\mathcal{W}_{j,\text{o}}^+$ for the smoothed scaling and wavelet functions just as we did for the HM wavelets: the smoothed mother wavelets are both supported in an interval of length two, one is symmetric and the other is antisymmetric (see Figure 4). The only difference is that the scaling functions both have support length two, so this time the antisymmetric scaling space also depends on the *antisymmetric* scaling function, not just the *internal* one as in the HM case.

PROPOSITION 4.3. *The expansion*

$$f = P_{\mathcal{V}_{1,o}^+} f + \sum_{j=1}^{\infty} \sum_{\omega_{ijk+} \in \mathcal{W}_{j,o}^+} \langle f, \omega_{jk-}^{i} \rangle \, \omega_{jk+}^{i}$$

holds for $H_0^1[0,1]$ and one has the norm equivalence

$$\|f\|_{H^1}^2 \sim \sum_{\varphi_{i1k} \in \mathcal{V}_{1,o}^+} |\langle f, \varphi_{i1k-} \rangle|^2 + \sum_{j=1}^{\infty} (1 + 2^{2j}) \sum_{\omega_{ijk+} \in \mathcal{W}_{j,o}^+} |\langle f, \omega_{ijk-} \rangle|^2$$

5. DIVERGENCE-FREE WAVELETS

5.1. Wavelets on $\mathbf{R^2}$

A general recipe for the divergence-free wavelets in any dimension can be found in [12] which also contains verification that the basis that we will write presently is indeed a basis for the appropriate space of divergence-free vector fields. We will restrict attention to two space dimensions here for the sake of illustration. There will be twelve divergence-free vector mother wavelets. In principle they are built by first building a biorthogonal tensor product wavelet basis for $L^2(\mathbf{R^2}, \mathbf{R^2})$ with smoothing in appropriate components – there will 24 mother wavelet components at this level – then obliquely projecting onto the divergence-free subspace, leaving twelve mother wavelet vector fields. We list the result in the Φ, Ψ notation:

Table 5.1: Divergence free and dual mother wavelets

Divergence-free wavelets	dual wavelet fields
$\vec{\Psi}_1 = (\Psi_{\tilde{s}+}(x)\Psi_{\tilde{s}}(y)^T, -\Psi_{\tilde{s}}(x)\Psi_{\tilde{s}+}(y)^T)$	$(\Psi_{s-}(x)\Psi_s(y)^T, 0)$
$\vec{\Psi}_2 = (-\Psi_{\tilde{s}+}(x)T_{M^*}\Phi_{\tilde{s}}^T(y), \Psi_{\tilde{s}}(x)\Phi_{\tilde{s}+}(y)^T)$	$(0, \Psi_s(x)\Phi_{s-}(y)^T)$
$\vec{\Psi}_3 = (\Phi_{\tilde{s}+}(x)\Psi_{\tilde{s}}(y)^T, -T_{M^*}\Phi_{\tilde{s}}(x)\Psi_{\tilde{s}+}(y)^T)$	$(\Phi_{s-}(x)\Psi_s(y)^T, 0)$

To clarify the notation, the $\vec{\Psi}_\nu$ are 2×2 matrices with values in divergence-free wavelets – recall that Ψ is regarded as a column vector. The component entries are the divergence-free mothers and the corresponding components of the duals are the dual mothers. Also, $\Psi_{\tilde{s}+}(x)$ is the result of smoothing $\Psi_{\tilde{s}}$, that is, $\Psi_{\tilde{s}+} = -\int \Psi_{\tilde{s}}$. Notice that the dual wavelets are not divergence-free. The divergence-free wavelets form a basis for $H^0(\mathrm{div}, \mathbf{R^2})$, the divergence-free subspace of the Sobolev space $H(\mathrm{div}, \mathbf{R^2})$ whose components are in $L^2(\mathbf{R^2})$ with divergence in $L^2(\mathbf{R^2})$. Notice that the wavelet components in $\vec{\Psi}_3$ are essentially the same as those in $\vec{\Psi}_2$, but with the variables in reverse. This is why we have only plotted eight vector fields for the divergence-free mothers in Figure 6: to visualize the $\vec{\Psi}_3$ components look at the $\vec{\Psi}_2$ components sideways.

5.2. Wavelets on $[\mathbf{0}, \mathbf{1}]^\mathbf{2}$

The next issue is how to build suitable bases for divergence-free spaces on domains. The spaces of immediate interest to us in terms of solving Navier-Stokes using appropriate wavelets include the space $H^0_\parallel(\mathrm{div}, [0,1]^2)$ consisting of those vector fields in $L^2[0,1]^2$ which are divergence-free inside the square and which have boundary traces that are parallel to the boundary. In terms of fluid flow, the boundary condition just says that there is no fluid passing through the boundary. The analytic definition of this space is nontrivial because one needs to specify the space in which the traces live. We refer to Temam[13] for details. What matters here is primarily that the wavelets form a basis for the trace space and that expansions at the boundary are consistent in a simple way with expansions inside. To provide an appropriate basis for this space we need to restrict to appropriate divergence-free vector fields along the boundary. We reason through this as follows. Let $\vec{F} \in H^0_\parallel(\mathrm{div}, [0,1]^2)$. Along the line segment $x = 0; 0 \le y \le 1$ we want $\vec{F}(0,y)$ to be parallel to the boundary, that is, $\vec{F}(0,y) = (0, f(0,y))$. Therefore the x-component of $\vec{F}$ should vanish as $x \to 0^+$ but the y-component is a nontrivial trace. This tells us that for those wavelet terms that straddle the boundary we should be using restrictions to $[0,1]$ of the *antisymmetric* wavelets along the x-direction in the x-component but we should be using *symmetric* restrictions at $x = 0$ in the y-component of $\vec{F}$. Similar considerations apply to the other sides of the square. Fortunately, the divergence-free basis that we chose for $\mathbf{R^2}$ is in complete sympathy with the desired boundary modifications. Consider, for example, $\vec{\Psi}_1 = (\Psi_{\tilde{s}+}(x)\Psi_{\tilde{s}}(y)^T, -\Psi_{\tilde{s}}(x)\Psi_{\tilde{s}+}(y)^T)$. The upper left component vector field is $(\psi_{1\tilde{s}+}(x)\psi_{1\tilde{s}}(y), -\psi_{1\tilde{s}}(x)\psi_{1\tilde{s}+}(y))$. The wavelet $\psi_{1\tilde{s}+}$ is supported on $[-1,1]$ and is odd at $x = 0$ so for the boundary terms we should replace $\psi_{1\tilde{s}+}(x)$ by $\omega^{\mathrm{o}}_{\tilde{s}+}(x) = 2\psi_{1\tilde{s}+}(x)\chi_{[0,1]}(x)$. On the other hand, $\psi_{1\tilde{s}}$ is even at $x = 0$ so we should replace it by $2\omega^{\mathrm{e}}_{\tilde{s}}$. *Consequently, the limit as $x \to 0^+$ of the wavelet expansion of $\vec{F}$ will be completely consistent with the expansion of the boundary trace $f(0,y)$ so long as the wavelet coefficients are suitably normalized by the value $\omega^{\mathrm{e}}_{jk\tilde{s}}(0)$.* Again, corresponding considerations apply to the other mother wavelet vectors and the other sides of the square.

To summarize: the process of boundary modifications of smoothed HM wavelets to obtain a basis for $H_0^1[0,1]$ can be coupled with the Lemarié/Strela process of manufacturing divergence-free wavelets to produce a wavelet basis for $H_{\|}^0(\mathrm{div},[0,1]^2) \cap (H_0^1[0,1] \otimes L^2[0,1], L^2[0,1] \otimes H_0^1[0,1])$ in such a way that wavelet expansions on the interior are completely consistent with wavelet expansions of boundary traces.

REFERENCES

1. M. Farge, N. K. R. Kevlahan V. Perrier and E. Goirand, "Wavelets and turbulence," *Proc. IEEE* **84**, pp. 639–669, 1996.
2. P. Federbush, "Navier and stokes meet the wavelet," *Comm. Math. Phys.* **155**, pp. 219–248, 1993.
3. K. Urban, "Wavelet bases in $h(\mathrm{div})$ and $h(\mathrm{curl})$," *preprint* , 1998.
4. G. Battle, P. Federbush and P. Uhlig, "Wavelets for quantum gravity and divergence-free wavelets," *Appl. Comp. Harm. Anal.* **1**, pp. 295–297, 1993.
5. P. G. Lemarié-Rieusset, "Un théorem d'inexistence pour les ondelettes vecteurs à divergence nulle," *C. R. Acad. Sci. Paris Sér. I Math.* **319**, pp. 811–813, 1994.
6. J. Lakey and M. C. Pereyra, "On the non-existence of certain divergence-free multiwavelets," *preprint* , 1998.
7. P. G. Lemarié-Rieusset, "Analyses multi-resolutions non orthogonales, commutation entre projecteurs et derivation et ondelettes vecteurs à divergence nulle," *Rev. Mat. Iberoamericana* **8**, pp. 222–237, 1992.
8. G. Donovan, J. Geronimo D. Hardin and P. Massopust, "Construction of orthogonal wavelets using fractal functions," *SIAM J. Math. Anal.* **27**, pp. 1158–1192, 1996.
9. D. Hardin and J. Marasovich, "Biorthogonal multiwavelets on $[-1,1]$," *preprint* , 1998.
10. V. Strela, *Multiwavelets: Theory and Applications.* Phd dissertation, MIT, 1996.
11. J. Lakey and M. C. Pereyra, "Divergence-free multiwavelets on rectangular domains," *preprint* , 1999.
12. J. Lakey, P. Massopust and M. Pereyra, "Divergence-free multiwavelets," in *Approximation Theory IX*, C. Chui and L. Schumaker, eds., pp. 161–168, Vanderbilt U. Press, Nashville, 1998.
13. R. Temam, *Navier Stokes Equations*, North Holland, Amsterdam, 1979.

Figure 1. Plots of HM scaling functions and wavelets and their duals for $s = 0$

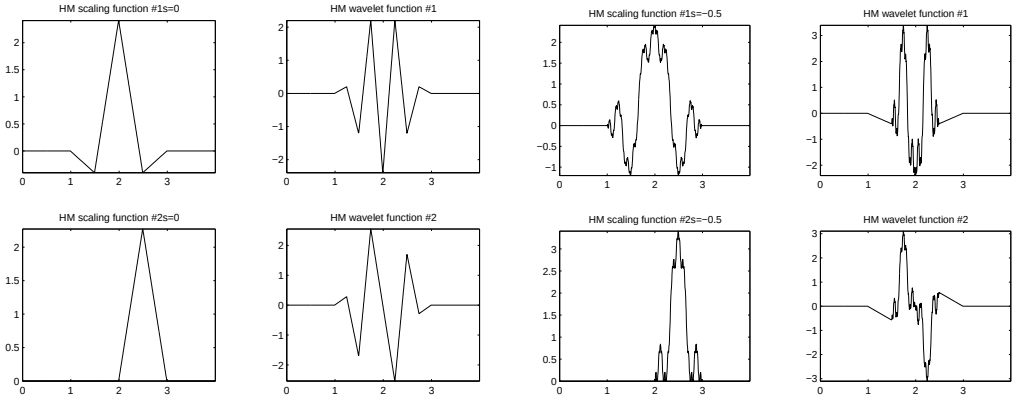

Figure 2. Plots of HM scaling functions and wavelets and their duals for $s = -1$

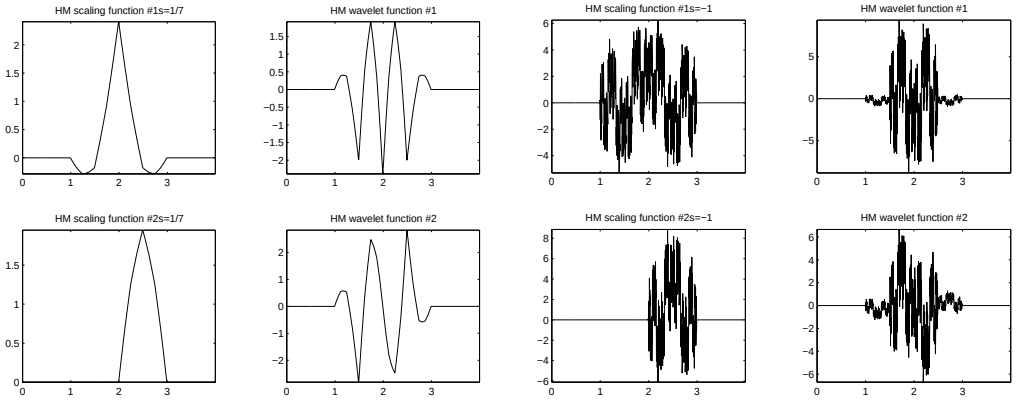

Figure 3. Plots of HM orthogonal scaling functions: $s = -1/5$ (DGHM) and $s = 1$

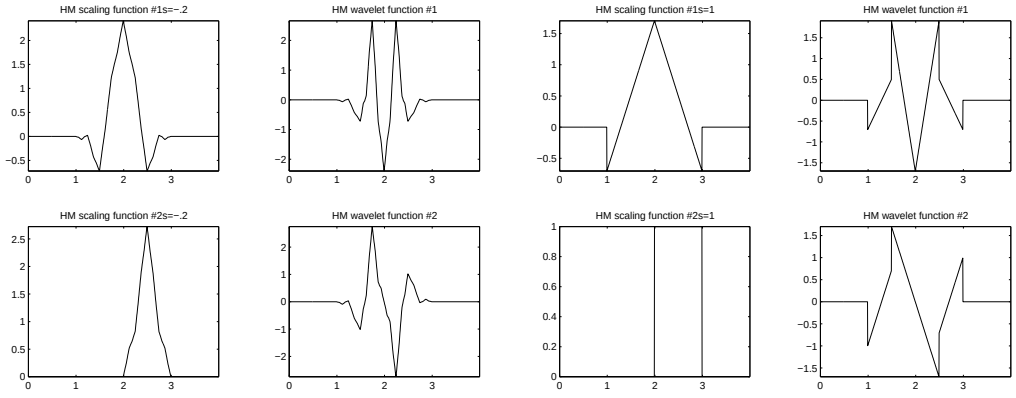

Figure 4. Biorthogonal smoothed and roughened versions for $s = 0$

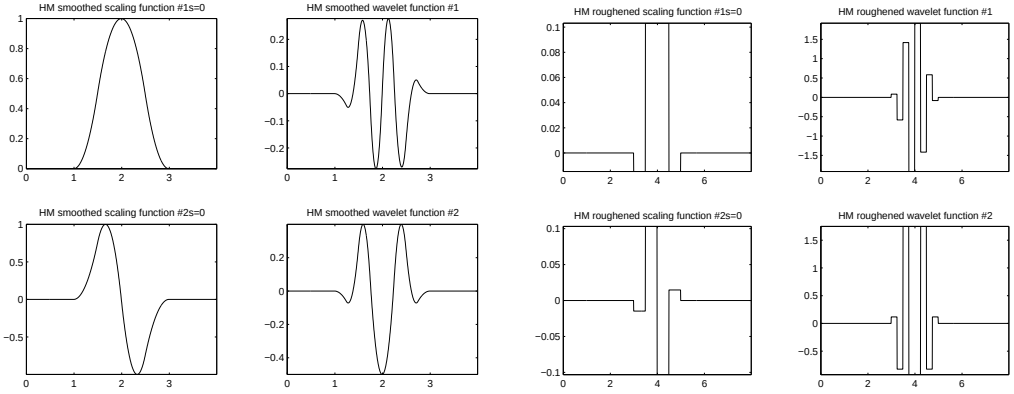

Figure 5. Biorthogonal smoothed and roughened versions for $s = -1/5$ (DGHM case)

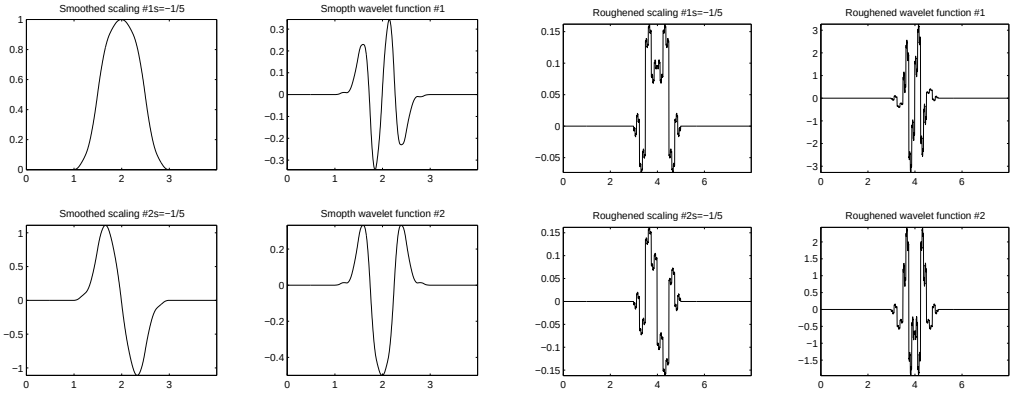

Figure 6. Divergence free mothers components for $\vec{\Psi}_1$ and $\vec{\Psi}_2$, supports not normalized